

See discussions, stats, and author profiles for this publication at: <https://www.researchgate.net/publication/8198385>

Bimolecular Homolytic Substitution (S_H2) Reactions with Hydrogen Atoms. Time-Resolved Electron Spin Resonance Detection in the Pulse Radiolysis of α -(Methylthio)acetamide

ARTICLE in JOURNAL OF THE AMERICAN CHEMICAL SOCIETY · DECEMBER 2004

Impact Factor: 12.11 · DOI: 10.1021/ja0458625 · Source: PubMed

CITATIONS

15

READS

93

4 AUTHORS, INCLUDING:



Pawel B Wisniowski

Instytut Chemii i Techniki Jądrowej

7 PUBLICATIONS 114 CITATIONS

SEE PROFILE



Krzysztof Bobrowski

Instytut Chemii i Techniki Jądrowej

129 PUBLICATIONS 2,020 CITATIONS

SEE PROFILE



Lily Hug

University of Greenwich

114 PUBLICATIONS 2,628 CITATIONS

SEE PROFILE

Bimolecular Homolytic Substitution (S_H2) Reactions with Hydrogen Atoms. Time-Resolved Electron Spin Resonance Detection in the Pulse Radiolysis of α -(Methylthio)acetamide

Pawel Wisniowski,^{†,‡} Krzysztof Bobrowski,[‡] Ian Carmichael,[†] and Gordon L. Hug^{*,†}

Contribution from the Radiation Laboratory, University of Notre Dame, Notre Dame, Indiana 46556, and Institute of Nuclear Chemistry and Technology, Dorodna 16, 03-195 Warsaw, Poland

Received July 9, 2004; E-mail: hug.1@nd.edu

Abstract: Pulse radiolysis of aqueous solutions of α -(methylthio)acetamide produced unexpectedly large quantities of acetamide radicals that were identified by time-resolved electron spin resonance (TRESR) spectroscopy. The pH dependence of the TRESR-measured radical yields, results from selective scavenging reactions, and density functional theory predictions of the reaction thermochemistry prove that bimolecular homolytic substitution, S_H2 , of the acetamide radical fragment by a H atom is the most likely formation pathway.

Introduction

One of the classic reaction pathways available to free radicals (R_1^\bullet) is bimolecular homolytic substitution (S_H2).¹



The most common reactions of this type are the simple radical abstractions occurring at monovalent centers (involving the removal of hydrogen or halogen atoms). However, more complex S_H2 mechanisms are also seen at multivalent atoms, usually at reactions sites with the capacity of behaving hypervalently. Work on such reactions was a very active area of research² among a small number of investigators in the 1960s and 1970s. In addition to the main body of this work that involved organic radicals, the early studies of S_H2 reactions included chemical systems where the reacting partners were multivalent metallic centers having low-lying unfilled orbitals.³

S_H2 reactions involving organic molecules with hypervalent atoms have also been studied extensively in the gas phase. There are examples of detailed experimental and theoretical studies^{4,5} of S_H2 radical processes at multivalent sites in the gas phase. These gas-phase investigations have been prevalent in the field of mass spectroscopy.⁶ On the other hand, in solution, recent

work on S_H2 reactions is more limited. In particular, bimolecular homolytic substitution reactions with the simplest free radical, containing a nucleus, the hydrogen atom, are almost nonexistent. For instance, in the 1988 comprehensive listing⁷ of H-atom rate constants with 574 compounds, there are only five S_H2 reactions^{8–10} listed that are not simple abstractions (hydrogen or halogen atoms).

Since hydrogen is the simplest radical with a nucleus, it is a useful probe for elucidating the mechanisms of solution-phase studies of S_H2 reactions at multivalent reaction centers. One convenient way to study the kinetics of hydrogen-atom reactions in solution is to generate them by the pulse radiolysis of aqueous solutions. The hydrogen atom is one of the principal radicals formed in the radiolysis of water.



Furthermore, at a low pH, the hydrated electrons (e_{aq}^-) from the radiolysis of water are converted through their reaction with protons into additional hydrogen atoms.



To look at hydrogen atoms directly, electron spin resonance (ESR)^{11–15} has been used. Furthermore, ESR can be used to

[†] University of Notre Dame.

[‡] Institute of Nuclear Chemistry and Technology.

- (1) Fossey, J.; Lefort, D.; Sorba, J. *Free Radicals in Organic Chemistry*; Wiley: Chichester, U.K., 1995.
- (2) Ingold, K. U.; Roberts, B. P. *Free-Radical Substitution Reactions*; Wiley-Interscience: New York, 1971.
- (3) Davies, A. G.; Roberts, B. P. Bimolecular homolytic substitution at metal centers. In *Free Radicals*; Kochi, J. K., Ed.; Wiley-Interscience: New York, 1973; Vol. I; pp 547–589.
- (4) Resende, S. M.; De Almeida, W. B. *J. Phys. Chem. A* **1997**, *101*, 9738–9744.
- (5) Syrstad, E. A.; Stephens, D. D.; Turecek, F. *J. Phys. Chem. A* **2003**, *107*, 115–126.
- (6) Turecek, F. Transient intermediates of chemical reactions by neutralization-reionization mass spectrometry. In *Topics in Current Chemistry*, Vol. 225: *Modern Mass Spectrometry*; Schalley, C. A., Ed.; Springer: Berlin, 2003.

- (7) Buxton, G. V.; Greenstock, C. L.; Helman, W. P.; Ross, A. B. *J. Phys. Chem. Ref. Data* **1988**, *17*, 513–886.
- (8) Navon, G.; Stein, G. *Isr. J. Chem.* **1964**, *2*, 151–154.
- (9) Jayson, G. G.; Stirling, D. A.; Swallow, A. J. *Int. J. Radiat. Biol. Relat. Stud. Phys. Chem. Med.* **1971**, *19*, 143–156.
- (10) Grachev, S. A.; Kropachev, E. V.; Litvyakova, G. I.; Orlov, S. P. *J. Gen. Chem. USSR* **1976**, *46*, 1813–1817 (English translation).
- (11) Eiben, K. H.; Fessenden, R. W. *J. Phys. Chem.* **1971**, *75*, 1186–1201.
- (12) Verma, N. C.; Fessenden, R. W. *J. Chem. Phys.* **1973**, *58*, 2501–2506.
- (13) Fessenden, R. W.; Verma, N. C. *Faraday Discuss. Chem. Soc.* **1977**, *63*, 104–111.
- (14) Han, P.; Bartels, D. M. *Chem. Phys. Lett.* **1989**, *159*, 538–542.
- (15) Bartels, D. M.; Mezyk, S. P. *J. Phys. Chem.* **1993**, *97*, 4101–4105.

follow any radicals generated as the products (R_2^*) in S_H2 reactions, such as in reaction 1.

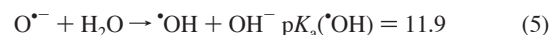
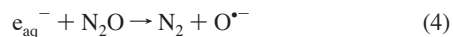
Because the sulfur atoms are hypervalent, they can form adducts with either the hydroxyl radical¹⁶ or the hydrogen atom,¹⁷ and furthermore, radical displacements at disulfides ($R-S-S-R'$) are a common method of producing thiyl radicals (RS^* or $R'S^*$).¹⁸ Early work in which thiols were detected as coming from H-atom reactions¹⁹ with ribonuclease was consistent with S_H2 reactions. In the present work, we look at the radiolysis of a sulfur-containing compound, α -(methylthio)acetamide, in acidic and neutral aqueous solutions and systematically investigate the source for the production of acetamide radicals. Time-resolved ESR (TRESR) is used to detect the acetamide radicals, and a recently developed method²⁰ is used to determine the radical yields via TRESR. Implications are drawn from the magnitude of these yields and from various scavenging experiments that lead to the conclusion that the acetamide radicals are indeed generated via an S_H2 reaction involving the hydrogen atom (not the hydroxyl radical) reacting with α -(methylthio)-acetamide.

Experimental Section

Materials. α -(Methylthio)acetamide was purchased from Parish Chemical Company (Orem, UT), sodium sulfite from Mallinckrodt, and acetamide (sublimed and zone-refined) from Aldrich. Tertiary butyl alcohol (*t*-BuOH) was purchased from Fisher. The pH 7 buffers were made with sodium phosphate monobasic and dibasic, both from Fisher. The low pH solutions were adjusted with $HClO_4$, from Aldrich, and the high pH solutions of acetylene dicarboxylic acid (Aldrich) and sodium sulfite were adjusted with NaOH or KOH (both from Fisher). Chemicals were used as received.

Methods. Radicals were generated via the radiolysis of aqueous solutions. The primary radicals from water (eq 2) were produced with 0.5 μ s pulses of 2.8 MeV electrons from a Van de Graaff accelerator. The radicals were detected with time-resolved electron spin resonance (TRESR).^{21–23} The ESR signals are not modulated, making it relatively straightforward to interpret the kinetic traces.^{24,25} Solutions were flowed through the irradiated quartz cell at a rate of about 10 mL/min. The quartz cell was located at the center of the resonant, transverse-electric (TE_{102}) cavity for X-band microwaves. The cell was irradiated edge-on, incident to a 0.4 mm face of the rectangular quartz cell. A bubble trap²⁶ was inserted into the flow system before the solution entered the quartz cell. The solution was also cooled so that the irradiations took place at approximately 15 °C. The relative irradiation doses were determined by measuring the current of the charges collected from the body of the cell. The concentration of $SO_3^{\cdot-}$ was determined by simulating the ESR kinetic traces, as described below. These concentrations, in turn, were compared to the current collected off the quartz cell, giving a relative measure of the dose delivered to the samples. In

more conventional terms, we also quote the radiation chemical yield (G in radicals per 100 eV of energy deposited or 0.1035 kJ/mol). The radiation chemical yield of $\cdot OH$ is $G(\cdot OH) = 2.82$.²⁷ However, in N_2O -saturated solutions ($[N_2O] \approx 25$ mM), the $\cdot OH$ yield is roughly doubled by the reaction of hydrated electrons ($G(e_{aq}^-) = 2.645$)²⁷ with N_2O .



Thus in N_2O -saturated aqueous solutions, the $SO_3^{\cdot-}$ radicals are formed from $\cdot OH$ oxidation of 5 mM sulfite solutions with a radiation chemical yield of $G = 5.47$ radicals per 100 eV of energy absorbed (0.567 μ M J^{-1}).²⁷ The other radiation chemical yield needed in this work is $G(H^*) = 0.57$.²⁷ These values are those of Elliot obtained at 25 °C.²⁷ At pH 1, the radiation chemical yield of $\cdot OH$ was 2.82, and the yield of H atoms was 3.22 because the hydrated electrons react with protons to give H^* radicals with a yield of $G(e_{aq}^-) = 2.645$ in addition to the primary yield of H atoms (0.57).

Determination of Radical Yields by ESR. The method of measuring yields of radicals by TRESR has been described previously in some detail.^{20,28} It is based on the notion that the observed ESR kinetic trace can be accurately simulated by the modified Bloch equations^{12,29} if an appropriate set of auxiliary experimental parameters is already known or can be measured. This set of parameters consists of the microwave magnetic field strength, H_1 , the line width, W , due to inhomogeneous broadening associated with the inhomogeneity in the external magnetic field, H_0 , and the spin relaxation times, T_1 and T_2 , of the various radicals.

The microwave magnetic field strength, H_1 , and the inhomogeneous line width, W , can be determined by measurements on the radical, $^{-}O_2CCH=C^{\cdot}CO_2^{-}$, formed by electron attachment to the dianion of acetylene dicarboxylic acid and followed by protonation of this radical trianion. The resulting $^{-}O_2CCH=C^{\cdot}CO_2^{-}$ radical is an extremely useful probe of the apparatus parameters H_1 and W because of its long electron spin relaxation times, $T_1 = 8.3$ μ s and $T_2 = 6.4$ μ s, as estimated below.

Using the $^{-}O_2CCH=C^{\cdot}CO_2^{-}$ radical as an instrumental probe with such long relaxation times has two major advantages. First, it is relatively easy to saturate the microwave transitions of such a radical, thereby, making it easy to produce Torrey oscillations.³⁰ The frequency of the Torrey oscillations is mainly dependent on H_1 when the external field, H_0 , is such that the spectrometer is pointing to the center of the microwave transition.³⁰ Thus, taking approximate values for T_1 , T_2 , and W from previous experiments,^{20,28} we simulated the high-field kinetic trace of the $^{-}O_2CCH=C^{\cdot}CO_2^{-}$ radical with an eye to match the frequency of the Torrey oscillations as H_1 was varied in the simulations of the kinetic trace. The simulations were computed by numerically integrating the modified Bloch equations.²⁵ The best match of the simulations to the kinetic trace was possible with $H_1 = 16$ mG at a microwave attenuation factor of -10 dB.

Having better values for H_1 , we can make a more accurate estimate of the inhomogeneous line width parameter, W . Again, for this experimental parameter, the long relaxation times, T_1 and T_2 , of the $^{-}O_2CCH=C^{\cdot}CO_2^{-}$ radical are an aid for measuring W since the homogeneous line width is narrow, making it easier to extract the inhomogeneous contribution. The empirical line shape was measured by recording a series of kinetic traces at external magnetic fields, H_0 , in the neighborhood of the transition, centered at $H_0 = H_c$, where H_c is the line's center in a conventional magnetic-field sweep. The ESR intensity was measured approximately 40 μ s after the radiolytic pulse, with the microwave attenuation set at -20 dB ($H_1 = 5.1$ mG). These conditions allowed us to use the Bloch formula for the line shape (slow

(16) McKee, M. L. *J. Phys. Chem. A* **2003**, *107*, 6819–6827.

(17) Sadilek, M.; Turecek, F. *Int. J. Mass Spectrom.* **1999**, *185–187*, 639–649.

(18) Asmus, K.-D.; Bonifacic, M. Sulfur-centered reactive intermediates as studied by radiation chemical and complementary techniques. In *S-centered Radicals*; Alfassi, Z. B., Ed.; Wiley: Chichester, U.K., 1999.

(19) Holmes, B. E.; Navon, G.; Stein, G. *Nature* **1967**, *213*, 1087–1091.

(20) Hug, G. L.; Fessenden, R. W. *J. Phys. Chem. A* **2000**, *104*, 7021–7029.

(21) Verma, N. C.; Fessenden, R. W. *J. Chem. Phys.* **1976**, *65*, 2139–2155.

(22) Fessenden, R. W.; Hornak, J. P.; Venkataraman, B. *J. Chem. Phys.* **1981**, *74*, 3694–3704.

(23) Madden, K. P.; McManus, H. J. D.; Fessenden, R. W. *Rev. Sci. Instrum.* **1994**, *65*, 49–57.

(24) Fessenden, R. W. *J. Chem. Phys.* **1973**, *58*, 2489–2500.

(25) Fessenden, R. W. Chemically induced electron polarization of radiolytically produced radicals. In *Chemically Induced Magnetic Polarization*; Muus, L. T.; Atkins, P. W.; McLauchlan, K. A.; Pedersen, J. B., Eds.; D. Reidel Publishing Co.: Dordrecht, The Netherlands, 1977; pp 119–150.

(26) Duncanson, I. B. *Fusion* **1993**, *40*, 26.

(27) Elliot, A. J. Rate constants and G-values for the simulation of the radiolysis of light water over the range 0–300 °C. Chalk River Laboratory, 1994.

(28) Wisniowski, P.; Carmichael, I.; Fessenden, R. W.; Hug, G. L. *J. Phys. Chem. A* **2002**, *106*, 4573–4580.

(29) Pedersen, J. B. *J. Chem. Phys.* **1973**, *59*, 2656.

(30) Torrey, H. C. *Phys. Rev.* **1949**, *76*, 1059.

passage).³¹ At the 40 μ s delay, the initial spin dynamics, associated with the tipping of the newly created spins in the H_1 field, was over, and at the low microwave power of -20 dB, there was little saturation of the microwave transition. The observed line shape, centered at H_c , was taken as a convolution of a Gaussian distribution of Bloch's slow-passage lines:

$$f(H) = N \sum_i \left(\frac{\exp\left(-2.77 \left(\frac{H_i - H_c}{W}\right)^2\right)}{\gamma_e^2 (H - H_i)^2 + T_2^{-2} + \gamma_e^2 H_i^2 \frac{T_1}{T_2}} \right) \quad (6)$$

Each of the slow-passage lines is centered at 1 of 21 local, time-independent external magnetic fields ($H_0 = H_i$). The Gaussian distribution represents the frequency of occurrence of radicals in an ensemble in which each radical is characterized by its local external field, H_i . In eq 6, γ_e is the gyromagnetic ratio of the electron, and W is the full-width at half-height of the Gaussian distribution of local magnetic fields, H_i , of radicals in the ensemble designed to account for inhomogeneity of the static field, H_0 .

After a first pass at computations for H_1 and W , as described above with the $^-\text{O}_2\text{CCH}=\text{C}^+\text{CO}_2^-$ radical, the process is refined by iterating the parameters, H_1 , W , and the spin relaxation times. Following such an iterative procedure, we obtained the values $H_1 = 16$ mG at a microwave attenuation factor setting of -10 dB, and $T_1 = 8.3$ μ s and $T_2 = 6.4$ μ s for the spin relaxation times of the $^-\text{O}_2\text{CCH}=\text{C}^+\text{CO}_2^-$ radical. The low pH and neutral pH experiments were performed at different dates with equipment repair, maintenance, and adjustments intervening. Particularly because of adjustments to the pole pieces of the electromagnet, the inhomogeneous line width changed slightly from 28.2 mG for the experiments at pH 1 to 23.5 mG for the experiments at neutral pH.

Once the inhomogeneous line width, W , and the microwave magnetic field strength, H_1 , have been determined from the analysis of the line shape and kinetic traces of the $^-\text{O}_2\text{CCH}=\text{C}^+\text{CO}_2^-$ radical, these two instrumental parameters can be used for the rest of the analysis. Before the final yield simulations can be determined, the spin relaxation times for the $\text{SO}_3^{\bullet-}$ radical and the acetamide radical are needed. Since both of these radicals have relatively fast spin relaxation, the assumption was made that $T_1 = T_2$ for both radicals; see, for example, the predictions of Redfield's theory in Slichter's book.³² Kinetic traces for both of these radicals were collected as a function of the external magnetic field, H_0 , in the vicinities of their respective central transitions. The microwave power is set to -15 dB to minimize saturation in the case of the $\text{SO}_3^{\bullet-}$ radical. Just as those in the case for the $^-\text{O}_2\text{CCH}=\text{C}^+\text{CO}_2^-$ radical, line shapes for the $\text{SO}_3^{\bullet-}$ and the acetamide radicals were generated from the averaged ESR intensity in time windows at delays that were sufficiently long to be away from the initial spin dynamics associated with the radicals' formation, tipping of the net magnetization vector of the newly formed radicals in the H_1 field, and any electronic time constants. (All of these factors are taken into account in the subsequent simulations of the kinetic traces using the modified Bloch equations.) The spin relaxation times for the $\text{SO}_3^{\bullet-}$ and the acetamide radicals were determined by matching these experimental line shapes with simulations of line shapes using eq 6 along with the appropriate H_1 and W , previously determined from the $^-\text{O}_2\text{CCH}=\text{C}^+\text{CO}_2^-$ experiments. From the simulations, $T_1 = T_2 = 1.5$ μ s for $\text{SO}_3^{\bullet-}$ and $T_1 = T_2 = 2.2$ μ s for the acetamide radical.

The heart of the ESR/radical yield method is to establish a "scale factor" to relate the magnitude of the ESR signal to the amplitude of the magnetization. The method, used here, is to relate these two

magnitudes through the observed *kinetic trace at the center* of an ESR line, not to the more straightforward method of comparing areas under the lines. However, the amplitude at the center of the observed line does not come only from radicals that are exactly on resonance with the external field because of the inhomogeneous broadening of the lines. For instance, an individual spin might be located at a point in the sample where the local magnetic field deviates from that experienced by the spins in fields close to the center of the distribution of local magnetic fields. This spin will have an off-resonance contribution to the observed ESR kinetic trace at $H_0 = H_c$ since the external magnetic field that it experiences ($H_0 = H_i$) is different from those of the spins at the center of the Gaussian distribution of the sample. In this sense, the kinetic trace at the center of the line is really sampling the whole line shape, and thus, is more analogous to the area under the ESR intensity profile than it is to the intensity at the maximum of the line. The advantage of the kinetic method for determining radical yields, by simply taking areas under the ESR lines, is that saturation of the microwave transitions is automatically taken into account by the modified Bloch equations.

This methodology of accounting for off-resonance contributions is why we can use the scale factor obtained from the simulation of the kinetic trace of the $\text{SO}_3^{\bullet-}$ line as a scale factor for the yield of spins. The scale factor from $\text{SO}_3^{\bullet-}$ is associated with the full yield of $^{\bullet}\text{OH}$ radicals under the dose applied at the geometry of the cell and microwave and external magnetic fields. However, given that $\text{SO}_3^{\bullet-}$ has only a single line, any radical that reaches a full yield of $^{\bullet}\text{OH}$ radicals in N_2O -saturated aqueous solutions should have the same scale factor. However, radicals, with multiple lines, must have their scale factors multiplied by the appropriate degeneracy factors.

Radiation chemical yields are added to the simulation program as part of the initial conditions. Because of this incorporation of the radiation chemical yields into the equations, the scale factors for full yield should be the same as that in $\text{SO}_3^{\bullet-}$. This is true, in particular, when the modified Bloch equations are used for radicals derived from $^{\bullet}\text{OH}$. Using it for radicals from H atoms, works in the same manner as long as the appropriate radical yields are incorporated into the computational program.

Computational Details. Structures of the thioether precursors and the various radicals, as well as radical cations derived from them, were obtained by the density functional theory (DFT) using a local version of the Gaussian98 suite of programs.³³ All DFT calculations employed the B3LYP functional,³⁴ and optimizations used the standard 6-31 G* basis. The effect of the aqueous environment was approximated by a polarized cavity model³⁵ using the integral equation formalism.^{36,37} Charge and spin distributions were characterized by natural population analyses.³⁸ Magnetic properties were evaluated using a basis set previously constructed to predict reliable Fermi contact contributions to NMR spin-spin coupling constants,³⁹ with g -tensors derived from perturbation theory.⁴⁰

- (33) Frisch, M. J.; Trucks, G. W.; Schlegel, H. B.; Scuseria, G. E.; Robb, M. A.; Cheeseman, J. A.; Zakrzewski, V. G.; Montgomery, J. A., Jr.; Stratmann, R. E.; Burant, J. C.; Dapprich, S.; Millam, J. M.; Daniels, A. D.; Kudin, K. N.; Strain, M. C.; Farkas, O.; Tomasi, J.; Barone, V.; Cossi, M.; Cammi, R.; Mennucci, B.; Pomelli, C.; Adamo, C.; Clifford, S.; Ochterski, J.; Petersson, G. A.; Ayala, P. Y.; Cui, Q.; Morokuma, K.; Salvador, P.; Dannenberg, J. J.; Malick, D. K.; Rabuck, A. D.; Raghavachari, K.; Foresman, J. B.; Cioslowski, J.; Ortiz, J. V.; Baboul, A. G.; Stefanov, B. B.; Liu, G.; Liashenko, A.; Piskorz, P.; Komaromi, I.; Gomperts, R.; Martin, R. L.; Fox, D. J.; Keith, T.; Al-Laham, M. A.; Peng, C. Y.; Nanayakkara, A.; Gonzalez, C.; Challacombe, M.; Gill, P. M. W.; Johnson, B.; Chen, W.; Wong, M. W.; Andres, J. L.; Head-Gordon, M.; Replogle, E. S.; Pople, J. A. *Gaussian 98*; Gaussian, Inc.: Pittsburgh, PA, 2001.
- (34) Becke, A. D. *J. Chem. Phys.* **1993**, *98*, 5648–5652.
- (35) Barone, V.; Cossi, M. *J. Phys. Chem. A* **1998**, *102*, 1995–2001.
- (36) Cancès, E.; Mennucci, B.; Tomasi, J. *J. Chem. Phys.* **1997**, *107*, 3032–3041.
- (37) Cancès, E.; Mennucci, B. *J. Chem. Phys.* **2001**, *114*, 4744–4745.
- (38) Reed, A. E.; Weinstock, R. B.; Weinhold, F. *J. Chem. Phys.* **1985**, *83*, 735–746.
- (39) Carmichael, I. *J. Phys. Chem.* **1993**, *97*, 1789–1792.
- (40) Neese, F. *J. Chem. Phys.* **2001**, *115*, 11080–11096.

(31) Bloch, F. *Phys. Rev.* **1946**, *70*, 460–474.

(32) Slichter, C. P. *Principles of Magnetic Resonance*, 2nd ed.; Springer-Verlag: Berlin, 1978.

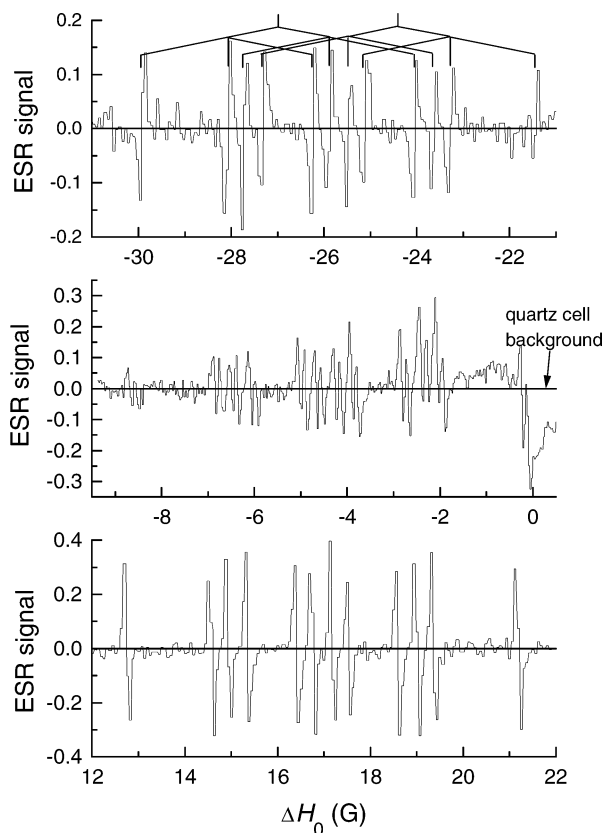


Figure 1. TRESR spectrum showing acetamide radicals from the pulse radiolysis of 2 mM aqueous solutions of α -(methylthio)acetamide, N_2O -saturated, at pH 1.2. The time window was 8.5–11.5 μs . The dose was such that [primary radicals] $\approx 32 \mu\text{M}$. The origin of the abscissa corresponds to the static magnetic field, H_0 , at which $g = 2.00\,043$, the hydrated electron's g -factor.

Results and Discussion

Spectral Identification. The TRESR spectrum following the pulse radiolysis of an N_2O aqueous solution of α -(methylthio)acetamide at pH 1 is shown in Figure 1. The time window for the spectrum is 8.5–11.5 μs after the 0.5 μs electron pulse. The spectrum is strongly polarized with the low-field lines in emission and the high-field lines in enhanced absorption.

The radical can be assigned by analyzing the splitting patterns. The three large groups of lines are separated by a hyperfine coupling constant of $a_{\text{H}} = 21.1 \text{ G}$. An analysis of the low-field lines is illustrated in Figure 1 with stick diagrams indicating additional hyperfine coupling constants of $a_{\text{H}} = 2.81$ and 2.35 G and $a_{\text{N}} = 1.9 \text{ G}$. A similar analysis applies to the central group of lines if the lines are considered to be doublets. The doubling of lines in the central band group, as well as a lack of doubling of the low- and high-field groups, is characteristic of second-order splitting⁴¹ associated with 1:2:1 patterns due to two magnetically equivalent protons with a large hyperfine coupling (i.e., $a_{\text{H}} = 21.1 \text{ G}$). The center of the spectrum is at a magnetic field offset, ΔH_0 , that computes into $g = 2.0030$. (The origin of the ΔH_0 scale corresponds to $g = 2.00043$, the center of the hydrated electron line.)⁴² The observed g -factor for the unknown transient and the hyperfine splittings have been previously reported and assigned to the acetamide radical, $\text{CH}_2\text{C}(\text{O})\text{NH}_2$.⁴³ From the computation methodology described

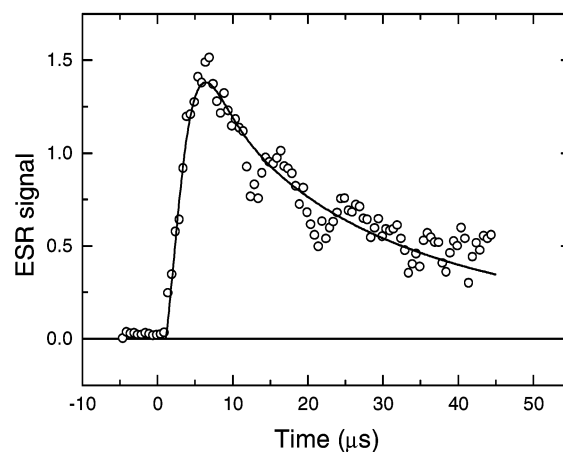


Figure 2. Pulse radiolysis of 5 mM aqueous solutions of α -(methylthio)acetamide, N_2O -saturated, at pH 1.2: TRESR kinetic trace of the central line ($\Delta H_0 = -5.03 \text{ G}$). The solid line is the kinetic simulation from the modified Bloch equations, with [primary radicals] = $29 \mu\text{M}$, $T_1 = T_2 = 2.2 \mu\text{s}$, $2k_2 = 2.2 \times 10^9 \text{ M}^{-1} \text{ s}^{-1}$, $k_1 = 2 \times 10^4 \text{ s}^{-1}$, $W = 28 \text{ mG}$, $H_1 = 16 \text{ mG}$, and “scale factor” = $0.26 \times 48 \text{ lines} \times \text{voltage sensitivity}$ ($0.2/0.5$) = 5.0, based on a full yield from H atoms. The reference scale factor = 5.7 for $\text{SO}_3^{\bullet-}$.

above, calculations gave $g = 2.00\,336$, $a_{\text{H}}(\text{CH}_2) = -21.2 \text{ G}$, $a_{\text{N}} = 0.9 \text{ G}$, and for the two inequivalent $-\text{NH}_2$ protons, $a_{\text{H}}(\text{NH}) = -1.9$ and -2.5 G . For additional confirmation of our assignment of the transient, the spectrum in Figure 1 was also obtained following the irradiation of an N_2O -saturated aqueous solution of acetamide at pH 7 (phosphate buffer). A similar TRESR spectrum was observed following pulse radiolysis of an N_2O -saturated aqueous solution of 5 mM α -(methylthio)acetamide at pH 7 (phosphate buffer).

Radical Yield Determination. The ESR lines appeared to be distinctly weaker at pH 7 compared to those at pH 1. If the $\text{CH}_2\text{C}(\text{O})\text{NH}_2$ radicals were *direct* successor radicals to the OH^\bullet radicals, then the opposite behavior would be expected. At pH 1, even in N_2O -saturated solutions, the hydrated electrons are rapidly converted into H^\bullet , by reaction 3, instead of into OH^\bullet radicals via eqs 4 and 5. Thus, the radiation chemical yield of OH^\bullet in N_2O -saturated solutions should be approximately twice as large at pH 7 compared to that at pH 1.

As an aid for tracking down the formation mechanism, the yields of $\text{CH}_2\text{C}(\text{O})\text{NH}_2$ from $\text{CH}_3\text{SCH}_2\text{C}(\text{O})\text{NH}_2$ were determined at both pH 1.2 and 7. Using the methodology described above, the results are $G = 2.5$ and 0.66 , respectively, taking Elliot's G for the primary radicals from water²⁷ listed in the Experimental Section. Figure 2 shows the kinetic trace of the $\text{CH}_2\text{C}(\text{O})\text{NH}_2$ radical at pH 1.2. The ESR line that is monitored is the lowest-field transition in the central group of lines (at $\Delta H_0 = -5.03 \text{ G}$). Central lines of ESR spectra are minimally polarized if the spin polarization is due to the radical pair mechanism.⁴⁴ Assuming OH^\bullet and H^\bullet , alternatively, are the precursor radicals, leads to yields of approximately 88 and 77%, respectively, based on the G values cited in the Experimental Section.

However, when the two analogous simulations were performed on the data at pH 7 (Figure 3), the yield of $\text{CH}_2\text{C}(\text{O})\text{NH}_2$ was 115%, assuming the sole precursor radical was H^\bullet , whereas the yield of $\text{CH}_2\text{C}(\text{O})\text{NH}_2$ was 12%, assuming

(41) Fessenden, R. W. *J. Chem. Phys.* **1962**, *37*, 747–750.

(42) Jeevarajan, A. S.; Fessenden, R. W. *J. Phys. Chem.* **1989**, *93*, 3511–3514.

(43) Livingston, R.; Zeldes, H. *J. Chem. Phys.* **1967**, *47*, 4173–4180.

(44) Adrian, F. J. *J. Chem. Phys.* **1971**, *54*, 3918–3923.

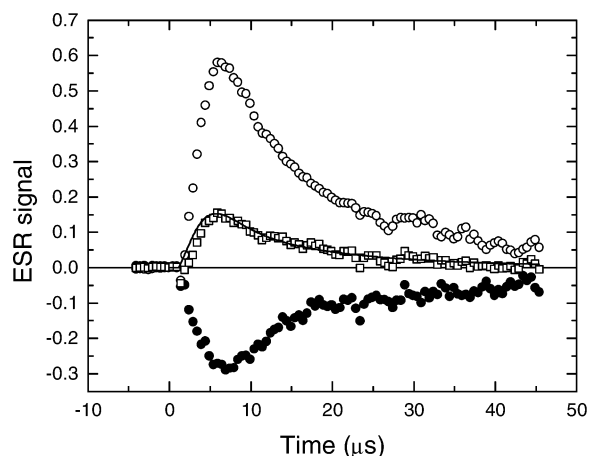


Figure 3. Pulse radiolysis of 5 mM aqueous solutions of α -(methylthio)acetamide, N_2O -saturated, at pH 7 (phosphate buffer). TRESR kinetic traces of two matching lines: high-field line (\circ) at $\Delta H_0 = 12.85$ G and low-field line (\bullet) at $\Delta H_0 = -21.66$ G, and the average of the two traces (\square). The solid curve is the kinetic simulation from the modified Bloch equations, with [primary radicals] = $40 \mu\text{M}$, $T_1 = T_2 = 2.2 \mu\text{s}$, $2k_2 = 2.2 \times 10^9 \text{ M}^{-1} \text{ s}^{-1}$, $k_1 = 5 \times 10^4 \text{ s}^{-1}$, $W = 23.5 \text{ mG}$, $H_1 = 16 \text{ mG}$, and scale factor = $0.0125 \times 48 \text{ lines} = 0.6$, based on a full yield from $\bullet\text{OH}$ radicals. The reference scale factor = 5.0 for $\text{SO}_3^{\bullet-}$.

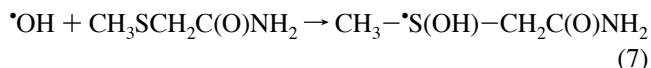
$\bullet\text{OH}$ as the sole precursor radical. The kinetic curve at pH 7 was an average of corresponding low- and high-field lines (Figure 3). Such a treatment should remove the anomalous polarization if it is due to like radicals involved in the radical pair mechanism.⁴⁴

The yield of $\bullet\text{CH}_2\text{C}(\text{O})\text{NH}_2$ at pH 1.2 was also measured with this same pair of lines. (The yield was determined, as described above, using only a single central line of the acetamide radical's spectrum.) The value determined from the average of the low- and (matching) high-field kinetic traces was 89% of the $\bullet\text{OH}$ yield or $G = 2.5$. Averaging the two independent (pH 1.2) measurements (one using a kinetic trace of a central line, and the second using the average of low- and high-field traces) of the yield of $\bullet\text{CH}_2\text{C}(\text{O})\text{NH}_2$ at pH 1.2, we determined that $G(\bullet\text{CH}_2\text{C}(\text{O})\text{NH}_2) = 2.5$ (89% of the $\bullet\text{OH}$ yield or 78% of the H^\bullet yield).

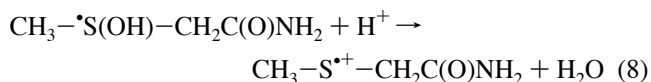
In both kinetic simulations of Figures 2 and 3, the radical–radical combination rate constant, $2k_2$, was $2.2 \times 10^9 \text{ M}^{-1} \text{ s}^{-1}$.⁴⁵ In the simulations of Figures 2 and 3, a pseudo-first-order component, k_1 , was included. This rate constant was consistent with that of the acetamide radical reacting with the substrate, with a bimolecular rate constant of $0.4\text{--}1.0 \times 10^7 \text{ M}^{-1} \text{ s}^{-1}$, and could correspond to H abstraction from the substrate by the acetamide radical. However, this is only tentative because the averaging of the kinetic traces (from matching high- and low-field traces) introduces large errors in the tail of the resulting kinetic traces due to the propagation of errors.⁴⁶

H^\bullet versus $\bullet\text{OH}$ as the Precursor Radical. The straightforward implication from the comparative yield measurements at the two pH values is that the acetamide radical has the H atom as its precursor. However, it needs to be determined whether $\bullet\text{OH}$ is still not a possible precursor because the decay of the $\bullet\text{OH}$ adduct at the sulfur is acid catalyzed. Thus, the $\bullet\text{OH}$ adduct can have different pathways for reactions in the pH regions

under consideration. It is expected that most of the $\bullet\text{OH}$ radicals will follow the usual pathway and form primarily hydroxy-sulfuranyl radicals⁴⁷

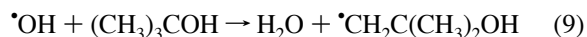


At a low pH, hydroxysulfuranyl radicals form sulfur-centered radical cations via



These monomeric sulfur-centered radical cations would decay by deprotonation,⁴⁸ which potentially yields both $\bullet\text{CH}_2\text{SCH}_2\text{C}(\text{O})\text{NH}_2$ and $\text{CH}_3\text{S}-\bullet\text{CH}-\text{C}(\text{O})\text{NH}_2$. The fate of these two α -thioalkyl radicals would likely be quite different. The first one, $\bullet\text{CH}_2\text{SCH}_2\text{C}(\text{O})\text{NH}_2$, could undergo β -scission to form the acetamide radical (see below). However, the $\text{CH}_3\text{S}-\bullet\text{CH}-\text{C}(\text{O})\text{NH}_2$ should be stabilized⁴⁹ by the captodative effect. On the other hand, at neutral pH, the fate of the hydroxysulfuranyl radical can be quite different.⁴⁹

Thus, to determine the source of the acetamide radical, a further series of experiments was performed. The first experiment used *tert*-butyl alcohol (*t*-BuOH) to preferentially scavenge $\bullet\text{OH}$ radicals.



The rate constant⁵⁰ for the reaction of *t*-BuOH with H^\bullet is $1.7 \times 10^5 \text{ M}^{-1} \text{ s}^{-1}$ and with $\bullet\text{OH}$ is $k_9 = 6 \times 10^8 \text{ M}^{-1} \text{ s}^{-1}$.⁷ Taking advantage of this divergence in rate constants, we compared the intensities of the high-field kinetic trace at $\Delta H_0 = 12.85$ G for two solutions only differing when 0.5 M *t*-BuOH was present or absent. Otherwise, the solutions were identical in that they both contained 2 mM α -(methylthio)acetamide, were at pH 1.2, and were nitrogen-saturated. In the solution with 0.5 M *t*-BuOH, only 1.3% of the $\bullet\text{OH}$ reacts with the α -(methylthio)acetamide, which is based on the competition of $\bullet\text{OH}$ for 2 mM α -(methylthio)acetamide ($2 \times 10^9 \text{ M}^{-1} \text{ s}^{-1}$)⁴⁹ and for 0.5 M *t*-BuOH. On the other hand, the yield of products from any reaction of α -(methylthio)acetamide with H^\bullet would only be limited by a time constant of about 12 μs based on the product of the above rate constant between H^\bullet and *t*-BuOH (0.5 M). The resulting traces show a reduction in the initial intensity of the kinetic trace of the acetamide radical (in the presence of *t*-BuOH) by about 70% of that in the absence of *t*-BuOH (Figure 4), but the tails of the kinetic traces are similar in intensity. A similar type of experiment at pH 2 and with 5 mM α -(methylthio)acetamide showed similar intensities in solutions with and without 0.5 M *t*-BuOH. These results are inconsistent with $\bullet\text{OH}$ being the precursor of acetamide radicals since only 1.3% of $\bullet\text{OH}$ is reacting with α -(methylthio)acetamide, and yet the yields of

(47) Bonifacic, M.; Möckel, H.; Bahnmann, D.; Asmus, K.-D. *J. Chem. Soc., Perkin Trans. 2* **1975**, 675–685.

(48) Mönig, J.; Goslich, R.; Asmus, K.-D. *Ber. Bunsen-Ges. Phys. Chem.* **1986**, *90*, 115–121.

(49) Wisniowski, P. Influence of functional groups on radiation induced radical processes in thioethers. Ph.D. Thesis, Institute of Nuclear Chemistry and Technology, Warsaw, Poland, 2001.

(50) Smaller, B.; Avery, E. C.; Remko, J. R. *J. Chem. Phys.* **1971**, *55*, 2414–2418.

(45) Hayon, E.; Iбата, T.; Lichtin, N. N.; Simic, M. *J. Am. Chem. Soc.* **1970**, *92*, 3898–3903.

(46) Bevington, P. R. *Data Reduction and Error Analysis for the Physical Sciences*; McGraw-Hill: New York, 1969.

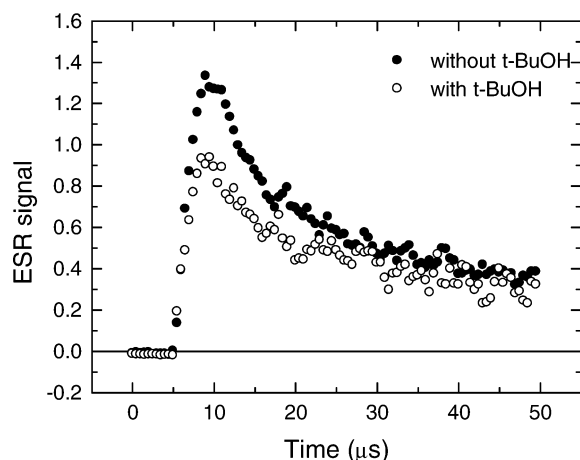
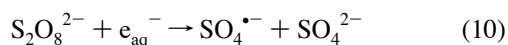


Figure 4. Pulse radiolysis of 2 mM aqueous solutions of α -(methylthio)acetamide, N_2 -saturated, at pH 1.2. TRESR kinetic traces at $\Delta H_0 = 12.85$ G. Open circles represent a solution with 0.5 M *t*-BuOH, and solid circles represent a solution without *t*-BuOH.

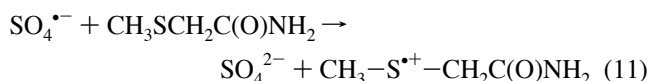
acetamide radicals are approximately the same with and without *t*-BuOH.

The two kinetic traces in Figure 4 are consistent with H^\bullet being the precursor of the acetamide radicals. The rate constant of H^\bullet reacting with α -(methylthio)acetamide is not known precisely, but in our Bloch simulations, a time constant on the order of microseconds was needed to fit the pseudo-first-order rise of the acetamide radical's ESR signal. (A formal bimolecular rate constant for the reaction of a H atom with this substrate would be $1.5\text{--}2 \times 10^8 \text{ M}^{-1} \text{ s}^{-1}$.) Qualitatively, this is consistent with the observed small decrease in the yield of the acetamide radical when *t*-BuOH is competing with α -(methylthio)acetamide for H^\bullet with the time constant of 12 μs , as computed above. The different initial intensities of the TRESR kinetic traces may also be a chemical-induced dynamic electron polarization effect related to different cross radical termination rate constants, reflecting the change in the nature of the radicals with different scavengers. Such changes in anomalous spin polarizations were seen due to changes in the cross reaction between H^\bullet and $^\bullet\text{OH}$ when *t*-BuOH was added.²⁵

Because preferential deprotonation of the sulfur-centered radical cation appeared to be an attractive alternative explanation for the appearance of the acetamide radicals (see discussion following eqs 7 and 8), we generated these sulfur-centered radical cations directly and looked for acetamide radicals. The sulfur-centered radical cations were formed via the oxidation of α -(methylthio)acetamide by $\text{SO}_4^{\bullet-}$ radicals. The $\text{SO}_4^{\bullet-}$ radicals were produced in the reaction of $\text{S}_2\text{O}_8^{2-}$ scavenging hydrated electrons.



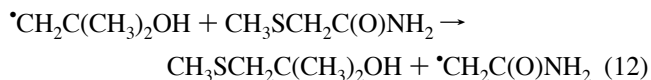
Care has to be exercised when doing experiments with peroxydisulfate since it can thermally oxidize organic species, but the solutions were used immediately after preparation. The reaction



was also observed⁴⁹ in pulse radiolysis with optical detection.

However, no TRESR signal due to the acetamide radical signal was observed at $\Delta H_0 = 12.85$ G following pulse radiolysis of a nitrogen-saturated aqueous solution of 0.5 M *t*-BuOH, 10 mM $\text{S}_2\text{O}_8^{2-}$, and 2 mM α -(methylthio)acetamide at pH 5.75. This is direct evidence that the acetamide radicals do not have the sulfur-centered radical cation as a precursor and is further (indirect) evidence that any acetamide radical formation via the $^\bullet\text{OH}$ radical is, at best, a minor pathway.

This particular experiment has another bearing on the question of the precursor of the acetamide radicals. Although the $^\bullet\text{CH}_2\text{C}(\text{CH}_3)_2\text{OH}$ radical, formed in the scavenging reaction (eq 9) of $^\bullet\text{OH}$ by *t*-BuOH, is normally not very reactive, it is conceivable that it could react with α -(methylthio)acetamide via an $\text{S}_\text{H}2$ reaction to form the acetamide radical.

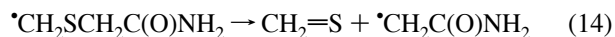


The lack of an ESR signal from acetamide radicals (in the above experiment with $\text{S}_2\text{O}_8^{2-}$ and 0.5 M *t*-BuOH) eliminates eq 12 as a source of the acetamide radicals also.

A third type of experiment also points to H atoms being involved in the formation pathway for the acetamide radicals. When an initially nitrogen-saturated aqueous solution of α -(methylthio)acetamide at pH 1.2 was subsequently saturated with oxygen, the original TRESR kinetic trace at $\Delta H_0 = 12.85$ G was significantly reduced in yield. Such a decrease in yield of acetamide radicals is expected if H atoms are their precursor since oxygen scavenges a significant amount of H atoms. Hydrogen atoms react rapidly ($2.1 \times 10^{10} \text{ M}^{-1} \text{ s}^{-1}$)⁷ with oxygen, which makes up for its small (~ 1.5 mM) concentration in water.

This set of three experiments eliminates $^\bullet\text{OH}$ as a precursor of the observed acetamide radicals from the radiolysis of aqueous solutions of α -(methylthio)acetamide and points to H atoms as the likely precursor of the observed acetamide radicals.

Formation Mechanisms. Since the experimental evidence points to the H atom as being the precursor of the acetamide radicals, we are faced with the need for an explanation of how acetamide radicals can be formed so efficiently from α -(methylthio)acetamide. The most likely reactions of H^\bullet with $\text{CH}_3\text{SCH}_2\text{C}(\text{O})\text{NH}_2$ would appear to be H abstraction. The formation mechanism for $^\bullet\text{CH}_2\text{C}(\text{O})\text{NH}_2$ would then be

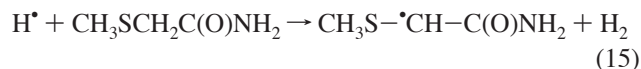


The driving force for reaction 14 is the double-bond formation. A similar β -scission reaction of aminyl radicals has been discussed in detail recently.⁵¹ β -Scission reactions, such as reaction 14, are the reverse of the radical polymerization of double-bonded monomers. In the two reactions above, the H abstraction in reaction 13, $\Delta G_{13} = -11.4$ kcal/mol, and the β -scission step of reaction 14, $\Delta G_{14} = +8.1$ kcal/mol, are from DFT calculations of the free energy changes. The two-step mechanism is not likely because of the endothermic step in reaction 14. However, a concerted reaction (combining steps

(51) Bonifacic, M.; Armstrong, D. A.; Carmichael, I.; Asmus, K.-D. *J. Phys. Chem. B* **2000**, *104*, 643–649.

13 and 14) would be spontaneous, but with only a small exothermicity, $\Delta G_{\text{concerted}} = -3.3$ kcal/mol.

Other H abstractions by H^\bullet , in competition with eq 13, would not lead in a straightforward manner to $\bullet\text{CH}_2\text{C}(\text{O})\text{NH}_2$. For instance, the radical $\text{CH}_3\text{S}-\bullet\text{CH}-\text{C}(\text{O})\text{NH}_2$ should be quite stable due to captodative effects.⁴⁹ The main competing H abstraction to reaction 13 is reaction 15.



Reaction 15 is about 11 kcal/mol more exothermic than reaction 13; so, $\Delta G_{15} = -22.7$ kcal/mol, by DFT calculations. Contrarily, the H abstraction of an amide hydrogen is slightly endothermic, with $\Delta G = +2.1$ kcal/mol, by DFT calculations.

On the other hand, a more direct reaction would be a free-radical substitution whereby the $\bullet\text{CH}_2\text{C}(\text{O})\text{NH}_2$ fragment of $\text{CH}_3\text{SCH}_2\text{C}(\text{O})\text{NH}_2$ is substituted with H^\bullet , forming a thiol. Reaction 16 is exothermic by a significant amount. From DFT, $\Delta G_{16} = -29.7$ kcal/mol.



This is an $\text{S}_{\text{H}}2$ reaction, a “bimolecular homolytic substitution”. It is driven by the strong S–H bond formation while only breaking a relatively weak C–S bond.

On the basis that activation energies follow the overall thermodynamics,⁵² the stepwise H abstraction– β -scission mechanism of reactions 13 and 14 is unlikely since the individual β -scission step 14 is distinctly endothermic. Even the concerted H abstraction– β -scission mechanism, with $\Delta G_{\text{concerted}} = -3.3$ kcal/mol, would not likely compete favorably with the H abstraction of reaction 15, with $\Delta G_{15} = -22.7$ kcal/mol. On the other hand, based solely on the thermodynamics, the $\text{S}_{\text{H}}2$ reaction 16 is the only thermodynamically favorable reaction, involving hydrogen atoms, that leads to the acetamide radical. This reaction appears to be the source of acetamide radicals from the radiolysis of aqueous solutions of α -(methylthio)-acetamide.

As mentioned in the Introduction, bimolecular homolytic substitutions with H atoms have not been extensively reported. However, the early work¹⁹ of Stein and his collaborators contains

reports of products containing –SH groups that formed in reactions of H atoms with proteins. This suggests that the H atoms were substituted for thiyl radicals $\text{R}-\text{S}^\bullet$. Recently, we identified that the $\text{S}_{\text{H}}2$ mechanism takes place when H atoms react with two other carbonyls, each containing thioethers.⁵³ These works, along with the finding in the present work, suggest that reactions of hypervalent sulfur compounds may have been overlooked in the studies that were mainly focused on the facile oxidation of these compounds that are so important in oxidative stress. Future work is planned to revisit the pulse radiolysis of such compounds in acidic solution in order to investigate the details of $\text{S}_{\text{H}}2$ reactions of these compounds with hydrogen atoms.

Conclusions

Acetamide radicals were identified in the pulse radiolysis of aqueous solutions of α -(methylthio)acetamide. The source of these radicals appears to be a bimolecular homolytic substitution ($\text{S}_{\text{H}}2$) of the acetamide radical fragment, in α -(methylthio)-acetamide, by hydrogen atoms. The yields of the acetamide radical tracked the H atoms' yields. Furthermore, controlled scavenging reactions, with *t*-BuOH and oxygen, point to H atoms as being the precursors of the acetamide radical. These same experiments eliminate $\bullet\text{OH}$ as being the precursor of the acetamide radical. A separate control experiment whereby sulfur-centered radical cations were formed directly, with no observed acetamide radicals, further eliminates the possibility that the acetamide radicals are formed from sulfur-centered radical cations, whether the sulfur-centered radical cations originate via $\bullet\text{OH}$ radicals or by other pathways.

Acknowledgment. This work was supported by the Office of Basic Energy Sciences of the U.S. Department of Energy. This paper is Document NDRL-4529 from the Notre Dame Radiation Laboratory. P.W. thanks the International Atomic Energy Agency for a predoctoral fellowship. G.L.H and P.W. are indebted to Professor R. W. Fessenden for extensive technical advice and assistance with TRESR, and the authors thank Professors D. A. Armstrong and K.-D. Asmus for discussions on β -scission.

JA0458625

(52) Evans, M. G.; Polanyi, M. *Trans. Faraday Soc.* **1935**, *31*, 875.

(53) Wisniowski, P.; Bobrowski, K.; Filipiak, P.; Carmichael, I.; Hug, G. L. *Res. Chem. Intermed.*, submitted.